High-Performance Carbon Nanotube Transparent Conductive Films by Scalable Dip Coating

Francesca Mirri, Anson W. K. Ma, Tienyi T. Hsu, Natnael Behabtu, Shannon L. Eichmann, Colin C. Young, Dmitri E. Tsentalovich, and Matteo Pasquali*

Department of Chemical and Biomolecular Engineering, Department of Chemistry, The Smalley Institute for Nanoscale Science and Technology, Rice University, 6100 Main Street, Houston, Texas 77005, United States

ABSTRACT

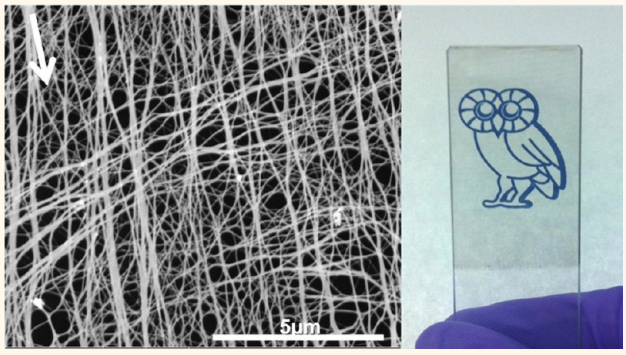

Transparent conductive carbon nanotube (CNT) films were fabricated by dip-coating solutions of pristine CNTs dissolved in chlorosulfonic acid (CSA) and then removing the CSA. The film performance and morphology (including alignment) were controlled by the CNT length, solution concentration, coating speed, and level of doping. Using long CNTs (~10 μm), uniform films were produced with excellent optoelectrical performance (~100 Ω/sq sheet resistance at ~90% transmittance in the visible), in the range of applied interest for touch screens and flexible electronics. This technique has potential for commercialization because it preserves the length and quality of the CNTs (leading to enhanced film performance) and operates at high CNT concentration and coating speed without using surfactants (decreasing production costs).

KEYWORDS: dip-coating · carbon nanotube · transparent conductive films · liquid crystals · flexible electronics

Since their discovery,[1] carbon nanotubes (CNTs) have received increasing attention due to their outstanding mechanical, thermal, and electrical properties.[2−6] In particular, research has focused on realizing in macroscopic objects the properties of single CNT molecules. CNTs have been formed into neat fibers[7−10] as well as thin conductive films.[11−13] In particular, transparent CNT films could replace indium tin oxide (ITO) because of their flexibility, resistance to flexural fatigue, and ease of manufacturing compared to the brittle ITO films, which must be fabricated by sputtering at low pressure or chemical vapor deposition at high temperature.[13] Moreover, CNT films may enable new applications in flexible electronics, because of their ability to bend repeatedly without cracking.[14,15]

Transparent conductive CNT films have been fabricated using a variety of processes that include dry and wet methods. The dry fabrication route consists of drawing films directly from CNT arrays.[16,17] Wet methods consist of dispersing the CNTs in a liquid and then fabricating films from the liquid phase. Multiple approaches have been used for wet method thin film assembly, including vacuum filtration,[11,18−20] drop-casting,[21] spin-coating,[22] rod-coating,[23] spray-coating,[24,25] and dip-coating.[26−28] Although the fluid phase approach is more conducive to industrial/commercial production, just a few of the above techniques (rod-, spray-, and dip-coating) are suitable for scale up and can be adapted to high-throughput coating processes such as slot, knife, slide, and roll coating.[29] Most liquid phase film fabrication methods rely on functionalization or the use of surfactants and sonication to form CNT dispersions. Functionalization degrades the electrical properties of the CNTs, disrupting the sp^2 bonds and yielding low film conductivity. Surfactant stabilization relies on sonication, which shortens the CNTs;[30] this also degrades film conductivity because it raises the number of CNT−CNT junctions per unit area of the film.[31] Moreover, good surfactants adsorb strongly on CNTs, and their removal from the film is difficult; surfactant residues in the final film increase sheet resistance.[32] Therefore, a solvent able to effectively disperse CNTs without damaging the

* Address correspondence to mp@rice.edu.

Received for review July 17, 2012 and accepted October 5, 2012.

Published online October 06, 2012
10.1021/nn303201g

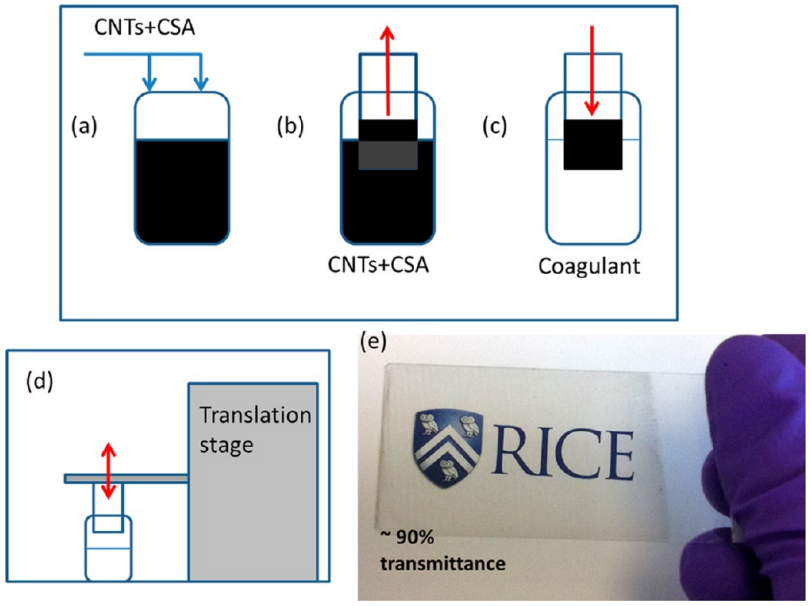

Figure 1. Schematic of the dip-coating process: (a) homogeneous solution of CNTs in chlorosulfonic acid; (b) withdrawal step and formation of the film on the glass slide by controlling the lifting speed; (c) coagulation and washing steps for the removal of CSA using a chloroform bath or a series of baths of chloroform coagulation followed by diethyl ether and water washes; (d) dip-coating setup; (e) 90% transparent thin film obtained by dip-coating from DWNT−CSA solutions.

ultimate properties of the films is needed. Chlorosulfonic acid (CSA) is a viable solution, and it circumvents the potentially detrimental effects of sonication, functionalization, and use of surfactants.[33,34] CSA-CNT solutions have already been used for SWNT film fabrication; however, these techniques were not scalable[35,36] or yielded poor film properties.[37,38]

This paper demonstrates the production of high-performance transparent conductive CNT films from CSA solutions by dip-coating. This is followed by CSA removal through a simple series of steps (coagulation or drying, followed by washing) that stabilizes the films and preserves the film structure after fabrication. This process is inherently scalable, and no sonication is needed; therefore, it can produce films consisting of $\sim$10 μm long CNTs, yielding excellent electrical properties. Film morphology and optical and electrical properties are controlled by the coating speed, CNT−CSA concentration, and level of doping.

RESULTS AND DISCUSSION

Thin films were fabricated starting from solutions of CNTs in CSA. Both HiPco single-walled carbon nanotubes (SWNTs) (length $L \sim 0.5\ \mu$m, diameter $D \sim 1$ nm)[33] produced at Rice University and double-walled carbon nanotubes (DWNTs) ($L \sim 10\ \mu$m, $D \sim 2.4$ nm) from Continental Carbon Nanotechnologies, Inc. (CCNI) were used (see Methods). SWNTs and DWNTs were dissolved (without sonication) in CSA at 1000, 2000, and 3000 ppm wt % (deposition from lower concentration solutions yielded sparse CNT coverage, high transparency $\sim$99.5%, and high sheet resistance $R_s \approx$ 12 kΩ/sq). Beyond a critical concentration w_l, CNTs form biphasic solutions with an isotropic (randomly oriented) phase in equilibrium with a nematic liquid crystalline phase.[34,39,40] This critical concentration scales inversely with CNT aspect ratio[41] as $w_l \approx D/L$. The measured transition concentrations were 4100 ppm for SWNTs[33] and 125 ppm for DWNTs; therefore, the SWNT solutions were isotropic, whereas the DWNT solutions contained a small amount of nematic phase ($\sim$10−20% depending on overall concentration; see Figure S1 in Supporting Information for images of SWNT and DWNT solutions). Glass slides were lowered into the CNT−CSA solution and were withdrawn at a controlled speed by a motorized arm (see Figure 1). Three methods were used to remove CSA from the films: (1) coagulation by immersion of the glass slide in chloroform ($CHCl_3$) followed by oven drying; (2) coagulation by immersion of the glass slide in chloroform, followed by washes in diethyl ether ($C_4H_{10}O$) and then water, with final oven drying; (3) direct evaporation of CSA in a vacuum oven at 150 °C followed by diethyl ether wash and drying as shown in previous literature.[37] Figure 1e shows an example of a 90% transmittance film fabricated using the dip-coating technique. All three methods yielded homogeneous films (Figure 2a) but different amounts of residual sulfuric acid (H_2SO_4) doping (see discussion below). Chloroform was chosen as the coagulant because it dissolves CSA without reacting (unlike water, which forms hydrochloric acid (HCl) gas and sulfuric acid), which can damage the film structure. Because of its high volatility, chloroform rapidly evaporates from the film once the slide is removed from the bath. However, chloroform is not a good solvent for sulfuric acid and

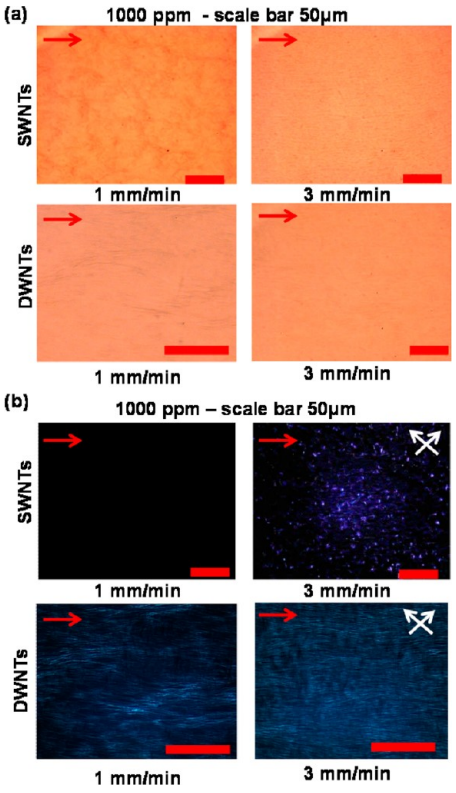

Figure 2. (a) Transmitted light micrographs of SWNT (top) and DWNT (bottom) films fabricated from a 1000 ppm solution at different withdrawal speeds. The scale bar is equal to 50 μm, and the red arrow represents the coating direction. (b) Polarized light micrographs of SWNT (top) and DWNT (bottom) films fabricated from a 1000 ppm solution at different withdrawal speeds (1 to 3 mm/min): SWNT films show isotropic orientation at low shear rate. Slightly ordered structures in the coating direction can be seen at 3 mm/min coating speed. DWNT films show a preferential orientation in the coating direction due to the liquid crystalline domains in the 1000 ppm CSA solution: these domains are stretched during dip-coating and yield ordered CNT bundles in the film (bright regions). The films were coagulated with chloroform (method 1). The scale bar is equal to 50 μm. The red and white arrows represent the coating direction and the cross polars, respectively.

hence leaves residual acid in the film. Washing in diethyl ether and water are necessary to remove sulfuric acid whenever sulfuric acid doping is not desired (as discussed below). The use of these three methods allowed the study of film electrical properties depending on the residual acid level.

SWNT and DWNT films displayed remarkably different morphology (Figure 2). Under cross-polarized light (Figure 2b), no ordered structure was observed in SWNT films coated at low speed (1−2 mm/min), whereas small birefringent regions are observable in films coated at higher speed (3 mm/min). Conversely, all DWNT films showed elongated birefringent domains aligned along the coating direction at all concentrations. This morphology is consistent with the microstructure of the coating solutions and the action of the shear field. In isotropic SWNT solutions, at low speed, the shear rate was insufficient to produce ordering in the films, whereas some shear-induced ordering was observed at high speed. Conversely, the pre-existing liquid crystalline domains in the DWNT solutions were stretched and aligned by the shear field.

Due to the CNT orientation, we expected the DWNT films to display anisotropic electrical properties.[42−44] We measured sheet resistance with a linear four-point probe at three different angles with respect to the coating direction and found no angular variation irrespective of the CSA removal technique (for example, a typical method 1 film had 117.0 ± 12.6, 117.8 ± 11.4, and 118.3 ± 8.0 Ω/sq at 0°, 45°, and 90°, respectively, at ~85% transmittance). Further study of the film morphology (Figure 3) using scanning electron microscopy (SEM) and transmission electron microscopy (TEM) leads to an explanation. The films consist of large bundles aligned along the coating direction (responsible for the optical birefringence) connected through a network of thinner bundles and individual CNTs predominantly aligned perpendicular to the large bundles. These perpendicular structures ensure isotropic film conductivity; they may arise from the isotropic phase present in the solution or be induced by vorticity aligning in the shear flow (known to occur in liquid crystalline polymers[45] and CNT fluids[39,46,47]).

The thickness, h_{wet}, of the dip-coated liquid film, called the wet film thickness, is controlled by the interplay of surface tension and gravity, which oppose film formation, and viscous forces, which draw liquid from the coating bath onto the substrate.[29,48,49] Whereas surface tension and gravity are process-independent, viscous forces can be controlled by the withdrawal speed u and solution CNT concentration (which affects viscosity). CNT concentration also affects the dry film thickness through $h_{wet} = h_{dry}\phi$, where ϕ is the CNT volume fraction in the coating liquid. Figure 4 shows how transmittance and sheet resistance (both related to the dry film thickness) change with withdrawal speed at different DWNT concentrations. As expected, higher withdrawal speed and higher CNT concentration yield thicker films (lower transmittance and lower sheet resistance). For Newtonian fluids, the relationship of wet film thickness to process parameters (the well-known Landau−Levich relation) is a function of the capillary number (ratio of viscous to surface tension forces),[29] or, in terms of velocity, $h_{wet} \approx u^{2/3}$. However, CNT solutions in CSA are non-Newtonian; in the range of measurements, they shear thin as power-law fluids with apparent viscosity $\eta_a = K\dot{\gamma}^{n-1}$, where $\dot{\gamma}$ is the shear rate, n is the power law exponent ($n = 1$ is a Newtonian fluid), and K is the consistency index (see rheology measurements in Supporting Information, Figure S2). Gutfinger and Tallmadge extended the Landau−Levich model to power-law fluids,[50] obtaining $h_{wet} \propto u^{2n/(2n+1)}$. Our film thickness data (Supporting Information, Figure S3) is closer to the Newtonian behavior, probably due to the low shear

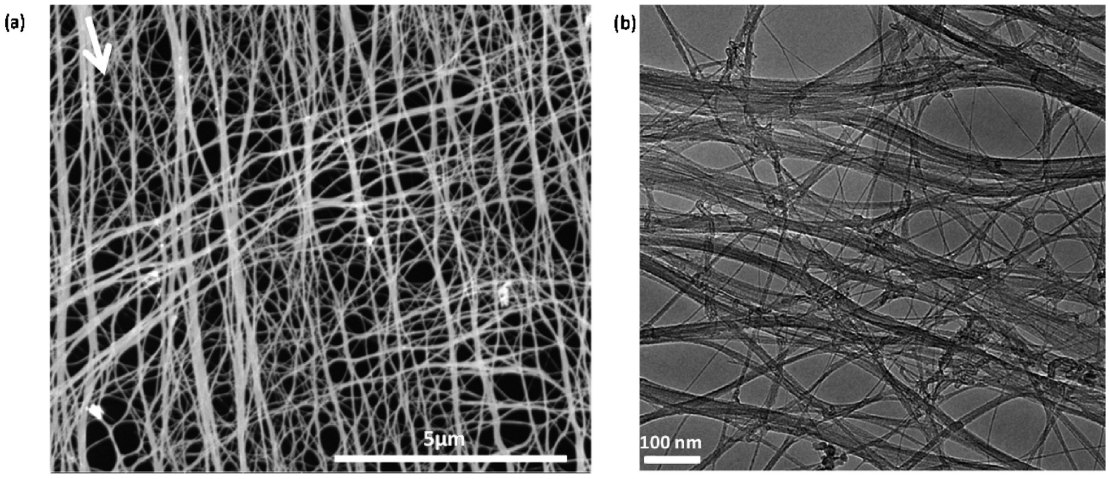

Figure 3. SEM images (a) and TEM images (b) of the films transferred onto TEM grids: the presence of an isotropic network of individual CNTs and bundles is probably responsible for the isotropic electrical properties of the films. The films were chloroform coagulated before being detached from the glass slide with a water bath.

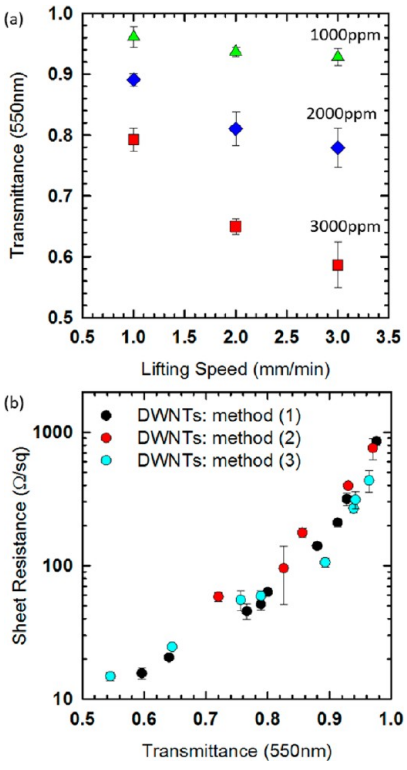

Figure 4. (a) Optical transmittance at the wavelength of 550 nm with respect to the withdrawal speed at different fixed concentrations of DWNT in CSA. Each value of transmittance is an average of 3 films fabricated with the same dip-coating parameters. (b) Optical transmittance *versus* sheet electrical resistance for films obtained by DWNTs using different acid removal processes. Films produced with direct CSA evaporation (method 3) and simple chloroform coagulation (method 1) showed lower sheet resistance values, most likely due to the presence of sulfuric acid (see XPS data in Supporting Information, Figure S4). On the other hand, higher values of sheet resistance were found for films coagulated with chloroform and washed with diethyl ether and water (method 2) due to the near complete removal of sulfuric acid.

rate at which the films are produced (shear thinning may influence the films produced at higher velocity).

Figure 4b shows sheet resistance *versus* transmittance: as expected, thicker films (lower transmittance) exhibit better electrical properties due to the increased number of pathways that the electrons can travel through. For films thinner than the wavelength of light, film transmittance T is related to sheet resistance by[18]

$$T = \left(1+\frac{Z_0}{2R_s}\frac{\sigma_{op}}{\sigma_{dc}}\right)^{-2} \quad (1)$$

where $Z_0 \approx 376.73\ \Omega$ is the characteristic impedance of vacuum, and σ_{op} and σ_{dc} are the optical and dc conductivity of the material, respectively. The ratio σ_{op}/σ_{dc} can be used to estimate film quality (lower values indicate better properties). In Figure 4b all the data fall on the same process curve, spanning ~2 orders of magnitude in sheet resistance, indicating that this simple coating process is very robust and versatile. Interestingly, film electrical properties depend on the fabrication technique used: the best electrical properties were obtained with films made by direct CSA evaporation and diethyl ether wash (method 3, yielding $\sigma_{op}/\sigma_{dc} \approx 0.039 \pm 0.008$), followed by chloroform-coagulated films (method 1, yielding $\sigma_{op}/\sigma_{dc} \approx 0.042 \pm 0.013$) and water-washed films (method 2, yielding $\sigma_{op}/\sigma_{dc} \approx 0.064 \pm 0.012$). The difference in electrical properties using the three techniques is related to the presence of sulfuric acid (H_2SO_4), which can be completely or partially removed from the film depending on the washing procedure. CSA reacts with the moisture in the air, leading to the formation of sulfuric acid, which acts as a doping agent.[23] Complete sulfuric acid removal was achieved by washing the films in water (method 2), while some residual sulfuric acid appeared in films produced using methods 1 and 3 (<0.1 atomic % for method 2, while methods 1 and 3 showed ~9.1 and 2.3 atomic % in sulfur content, respectively; these values were stable over ~90 days; see X-ray photoelectron spectroscopy

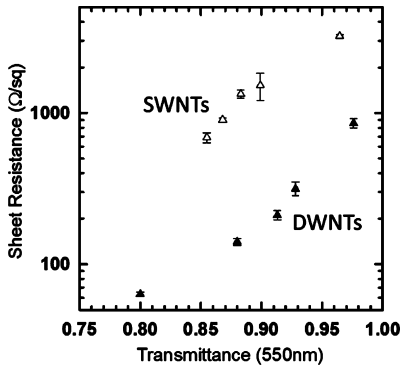

Figure 5. Transmittance *versus* sheet resistance for films obtained by DWNTs and SWNTs using simple chloroform coagulation (method 1): films obtained by SWNTs showed higher sheet resistance (from about 4 to 10 times higher) than DWNT films. The length of the CNTs plays a fundamental role in the film conductivity, as demonstrated in previous literature.[31] Each sheet resistance value represents the average of at least 5 random points in the film.

(XPS) data in Figure S4 in the Supporting Information). Although films made by different methods included various residual acid content, their stability in time was comparable. We observed day-to-day sheet resistance variations of up to ~20%, probably related to humidity fluctuations, but no long-term trend over a 90-day observation period (see Figure S5 in the Supporting Information). Interestingly, films made by methods 1 and 3 showed a rapid increase in sheet resistance (~40% and 21%, respectively) when a constant current of 1 mA was applied; this increase was reversible and is likely related to ionic conductivity due to residual sulfuric acid in the film (see Figure S6 in the Supporting Information).

Films fabricated from different CNTs are expected to exhibit different performance due to the respective quality, length, and diameter of the constituent CNTs. Although long CNTs are more difficult to disperse in liquids, they are desirable because the film conductivity scales as L^{δ}, where L is the average CNT length and δ is a constant close to 1 (in this work δ is about 1.12 for DWNT films and 1.49 for SWNT films; see Supporting Information).[31] When using CSA, length is not a barrier to dissolution.[33] We fabricated films of SWNT and DWNT; within the same fabrication method, SWNT films had ~4 to ~10 times higher sheet resistance than corresponding DWNT films (Figure 5), demonstrating the importance of the length and quality of CNTs for producing high-performance films; for example (method 1), at ~88% transmittance, SWNT and DWNT films have a sheet resistance of ~1300 and 140 Ω/sq, respectively, while at ~97% transmittance, SWNT and DWNT films have a sheet resistance of ~3200 Ω/sq ($\sigma_{op}/\sigma_{dc} \approx 0.371 \pm 0.073$) and 850 Ω/sq ($\sigma_{op}/\sigma_{dc} \approx 0.042 \pm 0.013$). In order to investigate the dependence of film conductivity on CNT length, percolation analysis was performed on the SWNT and DWNT films by fitting the measured sheet conductivity

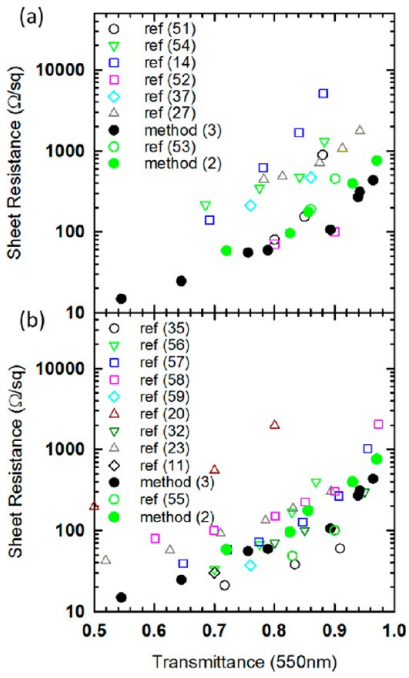

Figure 6. (a) Transmittance *versus* sheet resistance for films obtained by dip-coating in the recent literature.[14,27,37,51−54] (b) Transmittance *versus* sheet resistance of the best films obtained in the literature to date for various coating methods.[11,20,23,32,35,55−59] The values of sheet resistance reported represent the average of at least 5 random points in the film and were obtained for DWNT films with the three techniques used.

($\sigma(h_{dry}) = 1/R_s$) to the relationship[15]

$$\sigma(h_{dry}) = \sigma_0\left(\frac{h_{dry}}{h_c} - 1\right)^{\delta} \qquad (2)$$

(for details, see the Supporting Information and Figure S7). The fitted percolation exponent δ fell in the expected range (~1 to 1.5) for two-dimensional CNT networks.[15,31] The percolation threshold thickness h_c ≈ 5.3 nm for DWNT films was lower than the threshold for SWNT films ($h_c \approx 9.3$ nm), indicating that higher DWNT length contributed to the improved sheet resistance. However, the conductivity prefactor σ_0 was about 5-fold higher for DWNTs than SWNTs, indicating that intrinsic CNT conductivity may also account for the different performance.

Compared to CNT films in the dip-coating literature[14,27,37,51−54] (Figure 6a), our films from CSA−CNT solutions show excellent properties, likely due to the CNT length and quality as well as film morphology. Figure 6b compares our findings using methods 2 and 3 with the best values published in literature to date using various techniques.[11,20,23,32,35,55−59] The best performance was obtained by Hecht *et al.*,[35] who made DWNT films by filtration from CSA solutions, but reported short-term stability issues. The ~2× performance difference may be due to the absence of liquid crystalline domains in their low-concentration (~100 ppm) solutions, indicating that further improvements may be

attained by moving from dip-coating to premetered coating methods (which can operate at lower solid concentration and lower viscosity). These films show similar properties to those obtained by post-treatments with either nitric acid (HNO_3) or thionyl chloride ($SOCl_2$), known to dramatically improve the film properties by doping.[60,61] However, films doped by nitric acid or thionyl chloride have poor electrical stability in time,[60,61] whereas the films reported here show stable properties over ~3 months. One possible explanation is the acid may be entrapped inside the CNTs (as shown recently in ref 63) rather than adsorbed onto the CNTs.

CONCLUSIONS

In this work, we reported a potentially scalable method to produce CNT thin conductive films from CSA solutions without the use of surfactants, functionalization, or sonication. The film thickness and morphology were controlled by the coating speed, CNT solution concentration, and CNT length; CSA was removed by coagulation or drying followed by washing. The resulting films have excellent electrical and optical properties and are stable in time even in the presence of some residual acid doping. Long-term stability may be improved further by packaging the films into multilayer electrode assemblies, such as those typically used in displays and touch screens. Dip-coating is scalable and can be adapted to higher-throughput processes such as slot, slide, and roll coating and can be used with long CNTs to produce high-performance CNT films. Hence, solution coating from CSA could become the method of choice for fabricating transparent conductive CNT films for commercial applications.

METHODS

CNT Solution Preparation and Setup. Purified DWNTs were purchased from CCNI (batch X647H). HiPco SWNTs (batch 188.3) were produced at Rice University and purified according to literature methods.[62] The average length of DWNTs was estimated to be about 10 μm, and they were mostly few-walled nanotubes (single, double, and triple walls with an average wall number of 2.25 and an external diameter of about 2.4 nm). CSA was used as received (grade 99%, purchased from Sigma-Aldrich). The CNTs and CSA were initially mixed at ~10 000 ppm in a speed-mixer (DAC 150.1 FV-K, Flack Tek Inc). This stock solution was then diluted to the coating concentrations by further speed-mixing for 10 to 20 min, followed by stir-bar mixing for 24 h. Each film was coated on a glass slide previously cleaned with acetone (C_3H_6O) and then air-dried. A motorized stage (vertically mounted syringe pump, Harvard Apparatus PHD 2000) was used to immerse and lift the glass slide into and out of both the CNT−CSA solution and chloroform bath at prescribed speed. In the case of simple chloroform coagulation (method 1), the films was immersed in chloroform for at least 20 min to ensure complete removal of the CSA. Finally, the film was annealed at 115 °C for 30 min to improve their adhesion to the glass support. When the complete sulfuric acid removal was desired (method 2), the glass slide was first immersed in chloroform for 20 min after fabrication. Then, the glass slide was left in a diethyl ether bath for 3 min. After the ether washing, the film was annealed in the oven at 115 °C for 15 min to improve the adhesion to the glass slide. Finally, the glass slide was immersed in a water bath to remove the residual sulfuric acid. The process was completed with another 15 min in the oven at 115 °C to dry the film. The intermediate film annealing between diethyl ether and water wash is necessary to avoid the detachment of the film from the substrate. The CSA removal was also performed using direct CSA evaporation (method 3) as described elsewhere.[37] In brief, the film was heated in a vacuum oven at 150 °C after fabrication for 20 min. Then, the glass slide was immersed in a diethyl ether bath for 3 min and dried in the oven for another 10 min. The whole dip-coating and coagulation process was performed in a glovebox purged continuously with dry air in order to keep the moisture concentration less than 10%: the presence of water vapor could result in an exothermic reaction between the residual moisture and chlorosulfonic acid, which may affect the integrity of the films due to the generation of HCl gas. The film deposited on one side of the glass slide was wiped off before the transmittance measurements.

Characterization. The CNT film morphology was studied using a Zeiss Axioplan optical microscope. TEM images were captured using JEOL 2010. The TEM sample preparation was achieved by immersing the dip-coated slides into a DI water bath after chloroform coagulation and transferring the floating films onto a TEM grid. Films produced in this manner can be easily detached from the glass slide and transferred to other substrates. FEI quanta 400ESEM FEG was used to obtain the SEM pictures. The transmittance of the films at the wavelength of 550 nm was measured by a UV−vis spectrometer (Shimadzu UV-1800), while the sheet resistance was obtained with a linear four-point probe device (Jandel model RM3-AR). The XPS spectra and the rheology data were obtained using PHI Quantera XPS and AR2000eX (TA Instruments) with a concentric cylinder Couette geometry, respectively.

Conflict of Interest: The authors declare no competing financial interest.

Acknowledgment. This work was supported by Air Force Office of Scientific Research (AFOSR) grants FA9550-06-1-0207 and FA9550-09-1-0590, Air Force Research Laboratories (AFRL) agreement FA8650-07-2-5061, and the Robert A. Welch Foundation (C-1668).

Supporting Information Available: Micrographs of 1000 ppm solutions of SWNTs and DWNTs in CSA, rheology tests of DWNT solutions at 1000, 2000, and 3000 ppm, XPS data showing residual sulfur, films' electrical stability with time, and percolation analysis. This material is available free of charge *via* the Internet at http://pubs.acs.org.

REFERENCES AND NOTES

1. Iijima, S. Helical Microtubules of Graphitic Carbon. *Nature* **1991**, *354*, 56–58.
2. Ruoff, R. S.; Lorents, D. C. Mechanical and Thermal Properties of Carbon Nanotubes. *Carbon* **1995**, *33*, 925–930.
3. Treacy, M. M. J.; Ebbesen, T. W.; Gibson, J. M. Exceptionally High Young's Modulus Observed for Individual Carbon Nanotubes. *Nature* **1996**, *381*, 678–680.
4. Baughman, R. H.; Zakhidov, A. A.; de Heer, W. A. Carbon Nanotubes - the Route toward Applications. *Science* **2002**, *297*, 787–792.
5. Tans, S. J.; Devoret, M. H.; Dai, H. J.; Thess, A.; Smalley, R. E.; Geerligs, L. J.; Dekker, C. Individual Single-Wall Carbon Nanotubes as Quantum Wires. *Nature* **1997**, *386*, 474–477.

6. Yakobson, B. I.; Avouris, P. Mechanical Properties of Carbon Nanotubes. In *Carbon Nanotubes*; Springer-Verlag: Berlin, 2001; Vol. 80, pp 287–327.
7. Vigolo, B.; Penicaud, A.; Coulon, C.; Sauder, C.; Pailler, R.; Journet, C.; Bernier, P.; Poulin, P. Macroscopic Fibers and Ribbons of Oriented Carbon Nanotubes. *Science* **2000**, *290*, 1331–1334.
8. Behabtu, N.; Green, M. J.; Pasquali, M. Carbon Nanotube-Based Neat Fibers. *Nano Today* **2008**, *3*, 24–34.
9. Ericson, L. M.; Fan, H.; Peng, H. Q.; Davis, V. A.; Zhou, W.; Sulpizio, J.; Wang, Y. H.; Booker, R.; Vavro, J.; Guthy, C.; *et al.* Macroscopic, Neat, Single-Walled Carbon Nanotube Fibers. *Science* **2004**, *305*, 1447–1450.
10. Li, Y. L.; Kinloch, I. A.; Windle, A. H. Direct Spinning of Carbon Nanotube Fibers from Chemical Vapor Deposition Synthesis. *Science* **2004**, *304*, 276–278.
11. Wu, Z.; Chen, Z.; Du, X.; Logan, J. M.; Sippel, J.; Nikolou, M.; Kamaras, K.; Reynolds, J. R.; Tanner, D. B.; Hebard, A. F.; *et al.* Transparent, Conductive Carbon Nanotube Films. *Science* **2004**, *305*, 1273–1276.
12. Hu, L.; Hecht, D. S.; Grüner, G. Carbon Nanotube Thin Films: Fabrication, Properties, and Applications. *Chem. Rev.* **2010**, *110*, 5790–5844.
13. Hecht, D. S.; Hu, L. B.; Irvin, G. Emerging Transparent Electrodes Based on Thin Films of Carbon Nanotubes, Graphene, and Metallic Nanostructures. *Adv. Mater.* **2011**, *23*, 1482–1513.
14. Ng, M. H. A.; Hartadi, L. T.; Tan, H.; Poa, C. H. P. Efficient Coating of Transparent and Conductive Carbon Nanotube Thin Films on Plastic Substrates. *Nanotechnology* **2008**, *19*, 205703.
15. Harris, J. M.; Iyer, G. R. S.; Bernhardt, A. K.; Huh, J. Y.; Hudson, S. D.; Fagan, J. A.; Hobbie, E. K. Electronic Durability of Flexible Transparent Films from Type-Specific Single-Wall Carbon Nanotubes. *ACS Nano* **2011**, *6*, 881–887.
16. Zhang, M.; Fang, S. L.; Zakhidov, A. A.; Lee, S. B.; Aliev, A. E.; Williams, C. D.; Atkinson, K. R.; Baughman, R. H. Strong, Transparent, Multifunctional, Carbon Nanotube Sheets. *Science* **2005**, *309*, 1215–1219.
17. Feng, C.; Liu, K.; Wu, J. S.; Liu, L.; Cheng, J. S.; Zhang, Y. Y.; Sun, Y. H.; Li, Q. Q.; Fan, S. S.; Jiang, K. L. Flexible, Stretchable, Transparent Conducting Films Made from Superaligned Carbon Nanotubes. *Adv. Funct. Mater.* **2010**, *20*, 885–891.
18. Hu, L.; Hecht, D. S.; Grüner, G. Percolation in Transparent and Conducting Carbon Nanotube Networks. *Nano Lett.* **2004**, *4*, 2513–2517.
19. Green, A. A.; Hersam, M. C. Colored Semitransparent Conductive Coatings Consisting of Monodisperse Metallic Single-Walled Carbon Nanotubes. *Nano Lett.* **2008**, *8*, 1417–1422.
20. Parekh, B. B.; Fanchini, G.; Eda, G.; Chhowalla, M. Improved Conductivity of Transparent Single-Wall Carbon Nanotube Thin Films *Via* Stable Postdeposition Functionalization. *Appl. Phys. Lett.* **2007**, *90*, 121913.
21. Sreekumar, T. V.; Liu, T.; Kumar, S.; Ericson, L. M.; Hauge, R. H.; Smalley, R. E. Single-Wall Carbon Nanotube Films. *Chem. Mater.* **2003**, *15*, 175–178.
22. Meitl, M. A.; Zhou, Y. X.; Gaur, A.; Jeon, S.; Usrey, M. L.; Strano, M. S.; Rogers, J. A. Solution Casting and Transfer Printing Single-Walled Carbon Nanotube Films. *Nano Lett.* **2004**, *4*, 1643–1647.
23. Dan, B.; Irvin, G. C.; Pasquali, M. Continuous and Scalable Fabrication of Transparent Conducting Carbon Nanotube Films. *ACS Nano* **2009**, *3*, 835–843.
24. Majumder, M.; Rendall, C.; Li, M.; Behabtu, N.; Eukel, J. A.; Hauge, R. H.; Schmidt, H. K.; Pasquali, M. Insights into the Physics of Spray Coating of Swnt Films. *Chem. Eng. Sci.* **2010**, *65*, 2000–2008.
25. Kaempgen, M.; Duesberg, G. S.; Roth, S. Transparent Carbon Nanotube Coatings. *Appl. Surf. Sci.* **2005**, *252*, 425–429.
26. Spotnitz, M. E.; Ryan, D.; Stone, H. A. Dip Coating for the Alignment of Carbon Nanotubes on Curved Surfaces. *J. Mater. Chem.* **2004**, *14*, 1299–1302.
27. Jang, E. Y.; Kang, T. J.; Im, H. W.; Kim, D. W.; Kim, Y. H. Single-Walled Carbon-Nanotube Networks on Large-Area Glass Substrate by the Dip-Coating Method. *Small* **2008**, *4*, 2255–2261.
28. Song, Y. I.; Kim, G. Y.; Choi, H. K.; Jeong, H. J.; Kim, K. K.; Yang, C. M.; Lim, S. C.; An, K. H.; Jung, K. T.; Lee, Y. H. Fabrication of Carbon Nanotube Field Emitters Using a Dip-Coating Method. *Chem. Vap. Deposition* **2006**, *12*, 375–379.
29. Kistler, S. F.; Schweizer, P. M. *Liquid Film Coating: Scientific Principles and Their Technological Implications*; Chapman & Hall: New York, 1997.
30. Lucas, A.; Zakri, C.; Maugey, M.; Pasquali, M.; van der Schoot, P.; Poulin, P. Kinetics of Nanotube and Microfiber Scission under Sonication. *J. Phys. Chem. C* **2009**, *113*, 20599–20605.
31. Hecht, D.; Hu, L. B.; Gruner, G. Conductivity Scaling with Bundle Length and Diameter in Single Walled Carbon Nanotube Networks. *Appl. Phys. Lett.* **2006**, *89*, 133112.
32. Geng, H.; Kim, K. K.; So, K. P.; Lee, Y. S.; Chang, Y.; Lee, Y. H. Effect of Acid Treatment on Carbon Nanotube-Based Flexible Transparent Conducting Films. *J. Am. Chem. Soc.* **2007**, *129*, 7758–7759.
33. Parra-Vasquez, A. N. G.; Behabtu, N.; Green, M. J.; Pint, C. L.; Young, C. C.; Schmidt, J.; Kesselman, E.; Goyal, A.; Ajayan, P. M.; Cohen, Y.; *et al.* Spontaneous Dissolution of Ultralong Single- and Multiwalled Carbon Nanotubes. *ACS Nano* **2010**, *4*, 3969–3978.
34. Davis, V. A.; Parra-Vasquez, A. N. G.; Green, M. J.; Rai, P. K.; Behabtu, N.; Prieto, V.; Booker, R. D.; Schmidt, J.; Kesselman, E.; Zhou, W.; *et al.* True Solutions of Single-Walled Carbon Nanotubes for Assembly into Macroscopic Materials. *Nat. Nanotechnol.* **2009**, *4*, 830–834.
35. Hecht, D. S.; Heintz, A. M.; Lee, R.; Hu, L.; Moore, B.; Cucksey, C.; Risser, S. High Conductivity Transparent Carbon Nanotube Films Deposited from Superacid. *Nanotechnology* **2011**, *22*, 075201.
36. Behabtu, N.; Lomeda, J. R.; Green, M. J.; Higginbotham, A. L.; Sinitskii, A.; Kosynkin, D. V.; Tsentalovich, D.; Parra-Vasquez, A. N.; Schmidt, J.; Kesselman, E.; *et al.* Spontaneous High-Concentration Dispersions and Liquid Crystals of Graphene. *Nat. Nanotechnol.* **2010**, *5*, 406–411.
37. Saha, A.; Ghosh, S.; Weisman, R. B.; Martí, A. A. Films of Bare Single-Walled Carbon Nanotubes from Superacids with Tailored Electronic and Photoluminescence Properties. *ACS Nano* **2012**, *6*, 5727–5734.
38. Pasquali, M.; Hwang, W.-F.; Schmidt, H. K.; Behabtu, N.; Davis, V.; Parra-Vasquez, A. N. G.; Green, M. J.; Booker, R.; Young, C. C.; Fan, H. Neat Carbon Nanotube Articles Processed from Super Acid Solutions and Methods for Production Thereof. U.S. Patent Appl. 20110110843, 2011.
39. Davis, V. A.; Ericson, L. M.; Parra-Vasquez, A. N. G.; Fan, H.; Wang, Y. H.; Prieto, V.; Longoria, J. A.; Ramesh, S.; Saini, R. K.; Kittrell, C.; *et al.* Phase Behavior and Rheology of SWNTs in Superacids. *Macromolecules* **2004**, *37*, 154–160.
40. Rai, P. K.; Pinnick, R. A.; Parra-Vasquez, A. N. G.; Davis, V. A.; Schmidt, H. K.; Hauge, R. H.; Smalley, R. E.; Pasquali, M. Isotropic–Nematic Phase Transition of Single-Walled Carbon Nanotubes in Strong Acids. *J. Am. Chem. Soc.* **2005**, *128*, 591–595.
41. Green, M. J.; Parra-Vasquez, A. N.; Behabtu, N.; Pasquali, M. Modeling the Phase Behavior of Polydisperse Rigid Rods with Attractive Interactions with Applications to Single-Walled Carbon Nanotubes in Superacids. *J. Chem. Phys.* **2009**, *131*, 084901.
42. Fischer, J. E.; Zhou, W.; Vavro, J.; Llaguno, M. C.; Guthy, C.; Haggenmueller, R.; Casavant, M. J.; Walters, D. E.; Smalley, R. E. Magnetically Aligned Single Wall Carbon Nanotube Films: Preferred Orientation and Anisotropic Transport Properties. *J. Appl. Phys.* **2003**, *93*, 2157–2163.
43. Pint, C. L.; Xu, Y. Q.; Morosan, E.; Hauge, R. H. Alignment Dependence of One-Dimensional Electronic Hopping Transport Observed in Films of Highly Aligned, Ultralong Single-Walled Carbon Nanotubes. *Appl. Phys. Lett.* **2009**, *94*, 182107.

44. Zamora-Ledezma, C.; Blanc, C.; Puech, N.; Maugey, M.; Zakri, C.; Anglaret, E.; Poulin, P. Conductivity Anisotropy of Assembled and Oriented Carbon Nanotubes. *Phys. Rev. E* **2011**, *84*, 062701.
45. Kiss, G.; Porter, R. S. *Mechanical and Thermophysical Properties of Polymer Liquid Crystals*; Chapman & Hall: London, 1998.
46. Ma, A. W. K.; Mackley, M. R.; Rahatekar, S. S. Experimental Observation on the Flow-Induced Assembly of Carbon Nanotube Suspensions to Form Helical Bands. *Rheol. Acta* **2007**, *46*, 979–987.
47. Lin-Gibson, S.; Pathak, J. A.; Grulke, E. A.; Wang, H.; Hobbie, E. K. Elastic Flow Instability in Nanotube Suspensions. *Phys. Rev. Lett.* **2004**, *92*, 048302.
48. Ashmore, J.; Shen, A.; Kavehpour, H.; Stone, H.; McKinley, G. Coating Flows of Non-Newtonian Fluids: Weakly and Strongly Elastic Limits. *J. Eng. Math.* **2008**, *60*, 17–41.
49. Abedijaberi, A.; Bhatara, G.; G. Shaqfeh, E. S.; Khomami, B. A Computational Study of the Influence of Viscoelasticity on the Interfacial Dynamics of Dip Coating Flow. *J. Non-Newtonian Fluid Mech.* **2011**, *166*, 614–627.
50. Gutfinger, C.; Tallmadge, J. A. Films of Non-Newtonian Fluids Adhering to Flat Plates. *AIChE J.* **1965**, *11*, 403–413.
51. Saran, N.; Parikh, K.; Suh, D. S.; Munoz, E.; Kolla, H.; Manohar, S. K. Fabrication and Characterization of Thin Films of Single-Walled Carbon Nanotube Bundles on Flexible Plastic Substrates. *J. Am. Chem. Soc.* **2004**, *126*, 4462–4463.
52. Xiao, G. Z.; Tao, Y.; Lu, J. P.; Zhang, Z. Y.; Kingston, D. Efficient Fabrication of Highly Conductive and Transparent Carbon Nanotube Thin Films on Polymer Substrates. *J. Mater. Sci.* **2011**, *46*, 3399–3404.
53. de Andrade, M. J.; Lima, M. D.; Skakalova, V.; Bergmann, C. P.; Roth, S. Electrical Properties of Transparent Carbon Nanotube Networks Prepared through Different Techniques. *Phys. Status Solidi RRL* **2007**, *1*, 178–180.
54. Song, Y. I.; Yang, C. M.; Kim, D. Y.; Kanoh, H.; Kaneko, K. Flexible Transparent Conducting Single-Wall Carbon Nanotube Film with Network Bridging Method. *J. Colloid Interface Sci.* **2008**, *318*, 365–371.
55. Shin, D.; Lee, J. H.; Kim, Y.; Yu, S. M.; Park, S.; Yoo, J. A Role of HNO_3 on Transparent Conducting Film with Single-Walled Carbon Nanotubes. *Nanotechnology* **2009**, *20*, 475703.
56. Li, Z.; Kandel, H. R.; Dervishi, E.; Saini, V.; Biris, A. S.; Biris, A. R.; Lupu, D. Does the Wall Number of Carbon Nanotubes Matter as Conductive Transparent Material? *Appl. Phys. Lett.* **2007**, *91*, 053115.
57. Green, A. A.; Hersam, M. C. Processing and Properties of Highly Enriched Double-Wall Carbon Nanotubes. *Nat. Nanotechnol.* **2009**, *4*, 64–70.
58. Zhou, Y. X.; Hu, L. B.; Gruner, G. A Method of Printing Carbon Nanotube Thin Films. *Appl. Phys. Lett.* **2006**, *88*, 123109.
59. Nirmalraj, P. N.; Lyons, P. E.; De, S.; Coleman, J. N.; Boland, J. J. Electrical Connectivity in Single-Walled Carbon Nanotube Networks. *Nano Lett.* **2009**, *9*, 3890–3895.
60. Jackson, R.; Domercq, B.; Jain, R.; Kippelen, B.; Graham, S. Stability of Doped Transparent Carbon Nanotube Electrodes. *Adv. Funct. Mater.* **2008**, *18*, 2548–2554.
61. Barnes, T. M.; Blackburn, J. L.; van de Lagemaat, J.; Coutts, T. J.; Heben, M. J. Reversibility, Dopant Desorption, and Tunneling in the Temperature-Dependent Conductivity of Type-Separated, Conductive Carbon Nanotube Networks. *ACS Nano* **2008**, *2*, 1968–1976.
62. Xu, Y.; Peng, H.; Hauge, R. H.; Smalley, R. E. Controlled Multistep Purification of Single-Walled Carbon Nanotubes. *Nano Lett.* **2004**, *5*, 163–168.
63. Green, M. J.; Young, C. C.; Parra-Vasquez, A. N. G.; Majumder, M.; Juloori, V.; Behabtu, N.; Pint, C. L.; Schmidt, J.; Kesselman, E.; Hauge, R. H.; *et al.* Direct Imaging of Carbon Nanotubes Spontaneously Filled with Solvent. *Chem. Commun.* **2011**, *47*, 1228–1230.